Dominant role of thermal magnon excitation in temperature dependence of interlayer exchange coupling: Experimental verification

S. S. Kalarickal,* X. Y. Xu,† K. Lenz, W. Kuch, and K. Baberschke‡

Institut für Experimentalphysik, Freie Universität Berlin, Arnimallee 14, D-14195 Berlin, Germany

Ultrathin Ni/Cu/Co trilayers were deposited in ultrahigh vacuum and the ferromagnetic resonance measured *in situ* as a function of both, temperature and out-of-plane angle of the external field. The interlayer exchange coupling J_{inter} was then unambiguously extracted at various temperatures, entirely from the angular dependence of the resonance field positions. The temperature dependence of $J_{inter}(T)$ follows an effective power law $AT^n, n \approx 1.5$. Analysis of the scaling parameter A shows an oscillatory behavior with spacer thickness, as does the strength of the coupling at $T=0$. The results clearly indicate that the dominant contribution to $J_{inter}(T)$ is due to the excitation of thermal spin waves and follows recently developed theory closely.

I. INTRODUCTION

The ferromagnetic/normal metal/ferromagnetic ultrathin film trilayer is the fundamental component in multilayered giant magnetoresistive (GMR) materials. The parameter which governs the ferromagnetic (FM) and the antiferromagnetic (AFM) coupling in these trilayers, and hence the utility of the GMR material is the interlayer exchange coupling (IEC) parameter J_{inter}. Considerable work has been done at the $T=0$ level see, e.g., Refs. [1] and [2]. Though this parameter has been well studied, the dependence of J_{inter} on temperature T, an extremely important aspect, has been much debated upon and not yet clearly understood.[3–14]

To elucidate the basic trilayer structure used for the investigation in this work, a schematic diagram is shown in Fig. [1]. Trilayers studied to date have comprised of ferromagnetic layers with different anisotropies. Among others, such systems as Fe/Pd/Fe,[4] Ni/Cu/Ni with differing Ni thicknesses to ensure in-plane and normal-to-plane anisotropies,[15,16] or Co/Cu/Ni with both in-plane anisotropies have been studied.[11,12]

For uncoupled trilayers, one expects two ferromagnetic resonance (FMR) lines, corresponding to the two layers. When the interlayer exchange coupling is engaged, these two lines correspond to the so-called optical and acoustic resonance modes. Previous methods of determining the T dependence of J_{inter}, given by Lindner and Baberschke,[16] correlate the change in J_{inter}, with the shift of the FMR position H_{res} between that of the first layer and the H_{res} for the optical mode. A complete angular dependence of the FMR spectrum for each temperature was not taken. This method has the drawback that the explicit and complicated temperature dependence of the parameters that affect H_{res}, like the magnetization and the anisotropy of the two films, cannot be easily taken into account.

The work presented in this paper is a study on the Co/Cu/Ni system, with 1.8 monolayers (ML) Co, 6 ML of Cu spacer, and 7 ML Ni on Cu (001) substrate. The present work provides an investigation of the temperature dependence of J_{inter} entirely determined from the angular dependence of the ferromagnetic resonance positions for weakly FM coupled trilayers near the ordering temperature. The

$T^n, n \approx 1.5$ dependence of J_{inter} is very clear. This work also gives a different analysis of the data from Refs. [16] and [12] to provide a complete picture for small spacer thicknesses in the range of 4 to 9 ML.

The main motivation for this work lies in the ongoing debate regarding the different contributions to the temperature dependence of J_{inter}. Three different sources have been attributed to this dependence. Early discussions regarding IEC and its temperature dependence focused solely on the electronic band structure.[2,13] The softening of the Fermi edge at higher temperatures makes the coupling less effective. The second effect is the interface contribution, which uses the spin asymmetry of the electron reflection coefficient with increasing temperatures. In either of these contributions, the strong coupling between the spins, which is the signature of FM materials, have not been taken into account.[7] The temperature dependence due to this third contribution, i.e., the coupling within the individual layers, is manifest in the excitation of thermal spin waves. The decrease in the interlayer exchange coupling due to spin-wave excitation was calculated recently in Ref. [12]. To provide a background for the work presented in this paper, a brief overview of the theory is given below.

Schwieger and Nolting have used a microscopic Heisenberg model to calculate the temperature dependence of low-energy spin-wave excitations. The difference in the free energy for parallel and antiparallel orientation of magnetization in the two ordered layers contributes to the temperature dependence of J_{inter}. This basically depends on two parameters: (i) the direct exchange coupling J_{intra} *within* the ferromagnetic layer, yielding also its Curie temperature, and (ii) the interlayer exchange coupling J_{inter} *between* the two layers FM1 and FM2. The direct exchange between the spins in each FM layer J_{intra} is much stronger, being in the meV regime while the IEC coupling J_{inter} for weak coupling in trilayers with spacer thickness $d \approx 3–9$ ML, is in the μeV range. To extract the effect of the magnetic contributions alone for different spacer thicknesses, J_{inter} has been normalized to the parameter $J_0 \equiv J_{inter}(T=0)$. The authors of Ref. [14] have discussed J_{inter}/J_0 as a function of an effective $T^{1.5}$ power law. Figure [2] shows the temperature dependences affected by these two parameters, as described by Schwieger
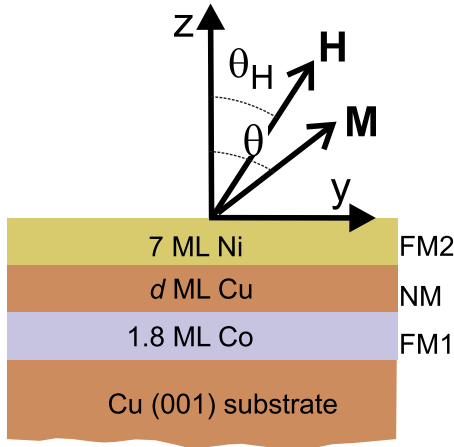
FIG. 1. (Color online) Geometry of the sample showing the relevant angles.

FIG. 2. Normalized J_{inter} as a function of $(T/300 \text{ K})^{1.5}$ for different parameters. (a) J_{inter}/J_0 for $J_{intra}=50$ and 90 meV and $J_0=40$ μeV, (b) J_{inter}/J_0 for $J_0=-22.5$ and 40 μeV and $J_{intra}=90$ meV. The data are taken from Ref. 14.

and Nolting.[14] Figure 2(a) shows the temperature dependence of J_{inter} normalized to J_0, for different J_{intra} values. This graph shows the influence of different ferromagnetic materials on the T dependence of J_{inter}. It is interesting to note that stronger direct exchange coupling in the FM layer results in a weaker temperature dependence for J_{inter}.

The effects due to different magnetic materials are not taken into account in this work where the investigated system comprises Co and Ni. However, it is important to note that $J_{inter}(T)$ also depends on the type of magnetic material used, which points at the competition between the thermal energy and the strength of the coupling. Figure 2(b) shows the T dependence of the normalized J_{inter} for different J_0 values. This also takes into account the properties of the spacer and interface at $T=0$. Overall, it can be seen that, an effective power law is followed. However, it is also clear that the results do not follow a straight line in $T^{1.5}$, i.e., the power is not exactly 3/2. The curvature and slope both depend on the parameters J_{intra} and J_0. It can be seen that the larger the J_0 value, the weaker the decrease of J_{inter} with T. This trend has been verified in the work presented in this paper.

All contributions due to the spacer, interface, and magnetic layers, nevertheless give an effective power-law dependence on the temperature,

$$J(T) \approx 1 - AT^n, \quad n \approx 1.5. \qquad (1)$$

As mentioned earlier, the differences between the above-mentioned mechanisms lie in their dependence on the spacer thickness. The spacer contribution, i.e., the electronic band-structure effect exhibits a linear dependence of A with d. The interface contribution is independent of d while the contribution due to spin-wave excitation gives a very weak dependence and oscillates with d. In connection with Fig. 2, it can be summarized that J_0 and the scaling parameter A should follow opposite trends as functions of spacer thickness.[14]

The interesting problem hence, lies in separating the T dependence of the above-mentioned mechanisms in ultrathin films. This question was partially addressed by Schwieger *et al.* for two AFM and one FM coupled trilayers.[11,12] For AFM coupled samples, it was found that the temperature dependence increases with coupling strength. However, no final conclusion could be made for the FM coupled samples and hence an overall picture was difficult to extract.
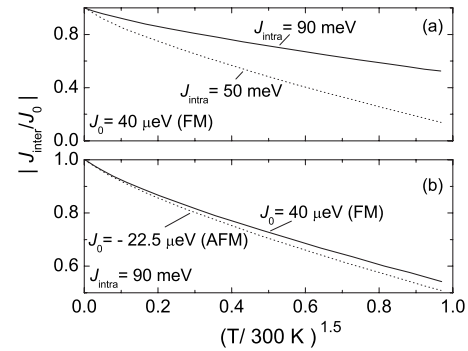
Another interesting aspect of nanomaterials is that the value of the Curie temperature T_c for these materials is very much below the bulk value and close to room temperature due to finite size effects.[17,18] Hence the study of the interlayer exchange coupling close to the ordering temperature gains importance. Ferromagnetic resonance with its well established theory gives a unique possibility to study the temperature dependence of J_{inter} in detail.

The paper is organized as follows. Section II presents the experimental and sample details as applicable to this paper and also gives some typical FMR data. Section III gives a short summary of the data analysis. Section IV presents the results and discussion and Sec. V gives the conclusions.

II. EXPERIMENTAL DETAILS AND FMR DATA

The *in situ* ultrahigh-vacuum (UHV) FMR spectrometer, and its capabilities have been described in detail elsewhere.[16,19] In brief, this setup allows one to deposit ultrathin, multilayered films and measure its FMR spectrum without any contact of the layers to air. The films that were investigated comprised of a few atomic monolayers. At these thicknesses, this technique becomes extremely crucial and useful since contact with air would change the magnetic properties of the film entirely. Also it is well known that the electronic band structure and the magnetic moment per layer for ultrathin films is different from bulk or even nanometer thick films.[20]

Trilayers were prepared on single crystalline Cu(001). The substrate was first Ar$^+$ ion sputtered at 3 kV, followed by a longer duration of sputtering at 1 kV. Subsequent annealing at 820 K for 10 min gave a better surface quality. First 1.8 ML of Co were deposited on Cu(001). Then 6 ML Cu spacer were deposited and the sample was annealed again at 420 K for 10 min. Recently, intermixing at the interface as a function of temperature has been discussed.[21] In the present experiment the sample undergoes a double cycle of annealing. This ensures that there is no further interdiffusion during the temperature-dependent measurements. Thereafter, FMR

spectra were recorded at various temperatures between 250 and 420 K at a microwave frequency of 9 GHz. The out-of-plane angular dependence of the FMR parameters was measured at room temperature. Then 7 ML of Ni were deposited on the spacer. The FMR measurements at various angles and temperatures were then repeated. The pressure during deposition and measurement was always in the low 10^{-10} mbar range. All depositions were done at room temperature. The thickness of the films was monitored using medium energy electron diffraction (MEED). Experiments were done on trilayers with Ni as the topmost layer and also for samples capped with 5 ML Cu. Samples were carefully annealed between the FMR scans to ensure that there are no adsorption effects which could bring about a change in the anisotropy. For this work, the thicknesses were chosen so that both the FM layers have an easy axis in the film plane.

As mentioned previously, a typical spectrum for a trilayer sample would comprise of two modes. The relative positions of the optical and the acoustic modes with respect to the modes for the uncoupled films, determine the type, FM or AFM, of the coupling.[15,16] At 320 K, the in-plane magnetized 1.8 ML Co layer with the 6 ML Cu cap, had the FMR position at $H_{res}=198$ Oe and a narrow FMR linewidth ΔH of 129 Oe. On the deposition of 7 ML Ni with a 5 ML Cu cap, the optical mode was found at 151 Oe while the acoustic mode was found at 1.9 kOe. The shift of H_{res} of the optical mode to a lower value with respect to the Co line, showed a weak FM coupling for this spacer thickness of 6 ML. The corresponding ΔH values were 250 Oe and 370 Oe.

A single Co film has a much lower ΔH than a Ni film. Note that in standard literature, it is shown that for larger coupling the intensity (oscillator strength) of the acoustic mode increases and the optical mode weakens.[16,22] Also, the optical mode has a larger relaxation rate than the acoustic mode.[16,22] Here, experimental evidence of the opposite limit, i.e., extremely weak coupling, is given. From the resonance positions one can clearly identify that the low field and narrow line is the optical mode while the higher field line and a broader line is the acoustic mode. The narrower line for the optical mode can easily be explained qualitatively. For the decoupled system, one has a narrow Co and a broad Ni resonance line. Now, when a weak coupling is switched on, the lines first shift to lower field positions. If the coupling was increased, the optical mode would have a larger ΔH than the acoustic mode. However, the nature of the coupling being so weak, the linewidths retained their comparative values.

Figure 3 shows the FMR profiles for two different out-of-plane external field angles θ_H. These profiles were taken on a trilayer with a 5 ML Cu cap, at room temperature. The figure shows the shift in the mode positions to higher field values for smaller θ_H values, as predicted by theory. The solid curves are fits to the data to two Lorentzian functions, which give the H_{res} and the ΔH measured as the width between the optima of the signal of the modes. For $\theta_H=90°$, the resonance positions were 0.138 and 1.88 kOe for the optical and the acoustic modes, respectively. The ΔH were 0.34 and 0.4 kOe, respectively. From a complete angular dependence of the resonance positions one can determine J_{inter}. Further details of extraction of J_{inter} from H_{res} versus θ_H will be evident from the next section and Fig. 6 below.
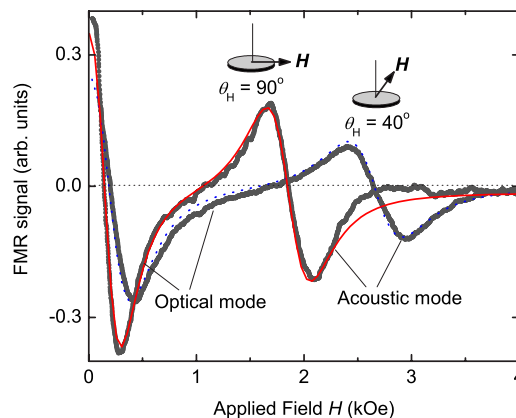
FIG. 3. (Color online) FMR profiles for two different angles of $\theta_H=90$ and 40°, taken at $T=307$ K for the capped sample. The blue dotted and red solid curves are fits to two coupled Lorentzians.

These angular dependences of FMR spectra were then taken at different temperatures in a range between 250 K and 420 K. As the temperature is reduced the spectra move to lower field values. This is because of the temperature-dependent changes in magnetization, anisotropy, and J_{inter} values. Below 250 K these changes pushed the spectra to such low fields that the optical mode was not visible. Hence the spectra for these temperatures could not be considered for analysis.

Figure 4 shows FMR profiles for different temperatures for $\theta_H=90°$. Figure 4(a) shows the profiles for an uncapped trilayer while Fig. 4(b) shows the profiles for a capped one. As before, the blue dotted and red solid curves are fits to the data to two Lorentzian functions. In both cases, the changes in the anisotropy energy and magnetization push the spectra toward higher fields as T is increased. Also, the linewidths of
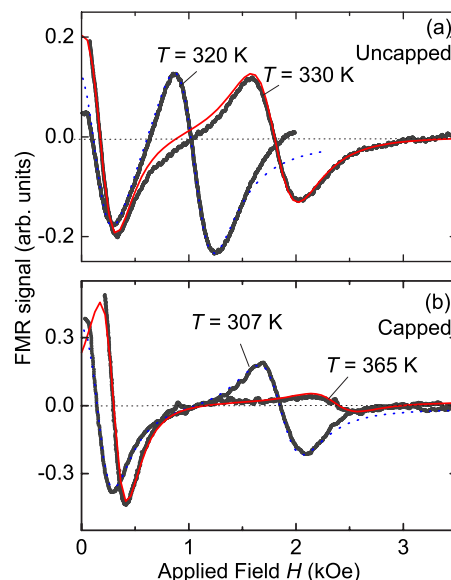
FIG. 4. (Color online) FMR profiles for different temperatures for $\theta_H=90°$. (a) Profiles at 320 K and 330 K for an uncapped sample. (b) Profiles at 307 K and 365 K for the capped sample. The blue dotted and red solid curves are fits to two coupled Lorentzians.

both the modes are seen to increase with temperature. It has been well documented that as one approaches T_c, the linewidth of a thin film is seen to increase.[23] This is also the case here since the T_c's of these layers are close to 400 K.[20]

The H_{res} and the linewidth at a particular θ_H and T were determined from the Lorentzian fits. Thereafter, at each temperature the complete out-of-plane angle dependence of H_{res} was fit to theory to give the J_{inter} parameter at that particular temperature.

III. FMR CONDITION FOR COUPLED TRILAYERS

The extraction of J_{inter} from the angular dependence of FMR spectra has been described in detail elsewhere.[16,19] For the sake of completeness, however, it is outlined in brief below. The resonance condition for a coupled trilayer system may be determined using the Smit and Beljers method,[24]

$$\left(\frac{\omega}{|\gamma|}\right)^2 = \frac{F_{\theta\theta}F_{\varphi\varphi} - F_{\theta\varphi}^2}{M^2 \sin^2 \theta}. \quad (2)$$

Here ω is the resonance frequency, $\gamma = g\mu_B/\hbar$ is the gyromagnetic ratio, and θ and φ are the azimuthal and the polar angles of the magnetization. F is the free energy density and the subscripts stand for second partial derivatives with respect to the angles. F includes the contributions due to the anisotropies and the interlayer exchange and is given by

$$F = F_{inter} + \sum_{i=1}^{2} F_i, \quad (3)$$

where

$$F_{inter} = -J_{inter}\frac{\mathbf{M}_1 \cdot \mathbf{M}_2}{M_1 M_2}, \quad (4)$$

$$F_i = d_i\left(-\mathbf{M_i} \cdot \mathbf{H} - (2\pi M_i^2 - K_{2\perp i}\sin^2 \theta_i)\right.$$

$$\left. - \frac{K_{4\|i}}{8}(3 + \cos 4\varphi_i)\sin^4 \theta_i\right). \quad (5)$$

Here, the subscript i stands for the two layers FM1 and FM2. $K_{2\perp}$ is the intrinsic out-of-plane anisotropy constant due to surface effects and tetragonal distortion of the film. The first nonvanishing contribution to the in-plane anisotropy is $K_{4\|}$, which is the fourfold in-plane anisotropy constant. The thicknesses of the individual layers are given by d_i. It is easy to see that the resultant expression for ω, albeit complicated, depends on the magnetizations and the anisotropies of the individual FM layers. At a glance, it may seem as if there are several fitting parameters. However, the power of the *in situ* UHV FMR spectrometer can be utilized to reduce these parameters drastically, since the layers can be deposited and measured step by step. The magnetization, anisotropies, and their temperature dependences for the first FM layer are estimated from the FMR measurements before the deposition of the second FM layer. Parameters for Co were obtained from the measurements taken of the Co layer prior to the deposition of Ni. For additional verification, 7
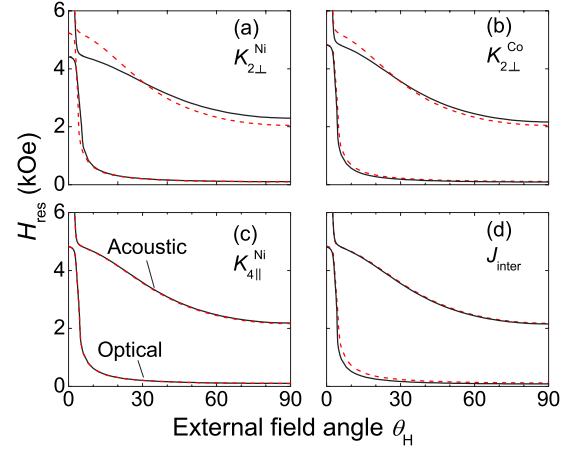
FIG. 5. (Color online) Calculated resonance positions as a function of θ_H. The simulations were done assuming $K_{2\perp}^{Ni}$ =6.9 μeV/atom, $K_{2\perp}^{Co}$=$-$69 μeV/atom, $K_{4\|}^{Ni}$=0.62 μeV/atom, and J_{inter}=2.8 μeV/atom. The black solid (red dashed) curves were obtained by varying one of the parameters by +10% ($-$10%). The varied parameter is indicated in each panel. The other parameters were kept fixed. From the simulation in panels (a) and (b) follows that the error bar for a fit of $K_{2\perp}$ is 1%. Having this value fixed the uncertainty for J_{inter} in panel (d) then is approximately 5%.

ML Ni were deposited separately on Cu(001) and the angular as well as the temperature dependences of FMR parameters were measured. This gives one a handle on all the fitting parameters required for the evaluation of J_{inter}. The g value for 7 ML Ni is very close to the bulk value while for 1.8 ML of Co, it is known that there is an enhancement in the orbital momentum and hence g was taken to be 2.21.[25] The $4\pi M_{eff}=4\pi M - 2K_{2\perp}/M$ values were taken to be 0.8 and 32.7 kG for Ni and Co, respectively.

The resonance positions as given from the above equations are obtained by numerical simulation. Figure 5 shows results of the simulations to illustrate the influence of each of the parameters for $K_{2\perp}^{Ni}$, $K_{2\perp}^{Co}$, $K_{4\|}^{Ni}$, and J_{inter} on $H_{res}(\theta_H)$. The curves being symmetric with respect to θ_H=0, the results are shown only for positive values of θ_H. The black solid (red dashed) curves were obtained by varying one of the parameters by +10% ($-$10%). The lower resonance field curves correspond to the optical mode. Several points are of note. First, a change in the $K_{2\perp}$ parameter for either Ni or Co brings about a change in both, the acoustic and the optical modes. Figures 5(a) and 5(b) show that the angular dependence of the acoustic mode is more sensitive to a change in $K_{2\perp}$ for either Ni or Co than the optical mode. Figure 5(c) shows the insensitivity of the angular dependence in either mode to a relative change in $K_{4\|}^{Ni}$. For all the fits to follow in this work, $K_{4\|}^{Co}$ was kept constant at zero. Figure 5(d) shows that the main effect of a relative variation of J_{inter} is seen on the optical mode. The effects taken together gave an estimated error of 10% in J_{inter}.

As was seen in Fig. 3, one can see that as the out-of-plane angle θ_H approaches zero, i.e., perpendicular to the film plane, H_{res} increases. This is more clearly understood from Fig. 6, which shows H_{res} vs θ_H at T=355 K. The solid red circles are the positions for the acoustic mode and the open
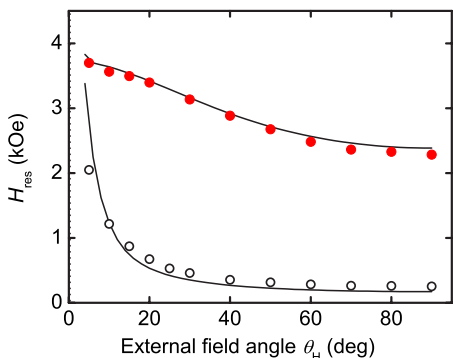
FIG. 6. (Color online) FMR resonance position vs the out-of-plane angle at $T=355$ K for the capped sample. The solid, red (open, black) circles are the data for the acoustic (optical) mode. The solid curves are fits to the data as described in the text.

black circles for the optical mode. The solid curves give a fit to the data according to the process described in the preceding section.

The variation of H_{res} with θ_H is dependent on three parameters, namely the magnetization, the anisotropy, and the interlayer exchange coupling. For this work, the values of the magnetization and the anisotropy were determined from the measurements taken on the single layers, as mentioned earlier. Taken together, the fit gives J_{inter} for the capped trilayer at 355 K to be 1.4 μeV/atom. This small value of J_{inter} for $d \approx 6$ ML has in fact been predicted by Bruno.[13]

IV. RESULTS AND DISCUSSION

The values of J_{inter} as obtained from the FMR data were analyzed as a function of temperature, and also compared to previously obtained results. With the results obtained here, a clear picture emerges regarding the temperature dependence of J_{inter} for both, FM and AFM coupling.

Figure 7 shows the values of J_{inter} vs spacer thickness at three different temperatures of 270 K, 300 K, and 365 K as indicated. The solid curve is a calculation according to
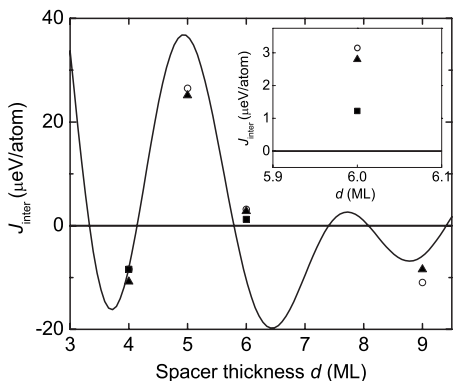
FIG. 7. J_{inter} vs spacer thickness at temperatures of 270 K (open circles), 300 K (solid triangles), and 365 K (solid squares). The solid curve is a calculation according to Bruno [Ref. 13]. The inset shows data for the capped sample with $d=6$ ML. The error is on the order of 10%.
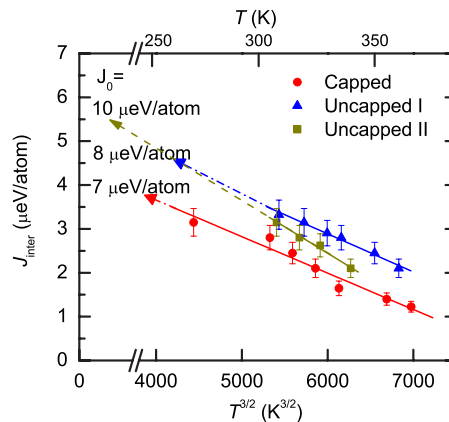
FIG. 8. (Color online) J_{inter} in absolute units vs $T^{3/2}$ for three 7 ML Ni /6 ML Cu/1.8 ML Co samples. The solid circles are the data for the capped sample while the solid triangles and squares are the data for the uncapped samples.

Bruno, which takes into account the effects due to Cu spacer[13] scaled on the y axis to match the data as is done in Ref. 16. The inset shows the data for the spacer thickness of 6 ML on an enlarged scale. The oscillations of J_{inter} have been previously discussed in Refs. 16 and 26 for these systems. These oscillations show the effect of the spacer thickness on J_{inter}. Here, the focus is on temperature dependence. The values for the calculations and the data for $d \neq 6$ ML have been taken from Lindner and Baberschke[16] and Schwieger et al.[12] The recent data are in concurrence with the previous results. The values of J_{inter} can be seen to decrease with increasing temperatures.

Figure 8 shows J_{inter} in absolute units of energy per atom, as a function of $T^{3/2}$ for three trilayer sets, the capped and two uncapped samples. The solid lines are linear fits to the data.[7] The values of T corresponding to the $T^{3/2}$ values are given on the top axis of the graph. The data sets can be seen to be linear in $T^{3/2}$. The uncapped trilayer samples have slightly higher values than the capped one. However, to set these on a similar scale, J_{inter} needs to be normalized to the zero intercept value of the linear extrapolation J_0, and studied as a function of temperature. These data can then be compared to previous observations in order to obtain a complete picture of the temperature dependence of J_{inter}.

Figure 9 gives the normalized J_{inter}/J_0 vs $T^{3/2}$ for different spacer thicknesses. The solid symbols are the data for $d=6$ ML, with the solid circles being the data for the capped and the squares and triangles being the data for the uncapped samples. These are compared with the data given in Refs. 12 and 16. The open triangles, open circles, and open squares are the data for spacer thicknesses of 4, 5, and 9 ML, respectively. These data were obtained by determining only two J_{inter} values from angular dependence and interpolating the others from the shift of the modes. Note that for the recent measurements the scatter and error bar of the data is larger because each value of J_{inter} was obtained independently, however it confirms the previous analysis in Refs. 12 and 16. With the results of these experiments, a complete picture emerges wherein one can compare the temperature dependences of FM as well as AFM coupling. The change for the
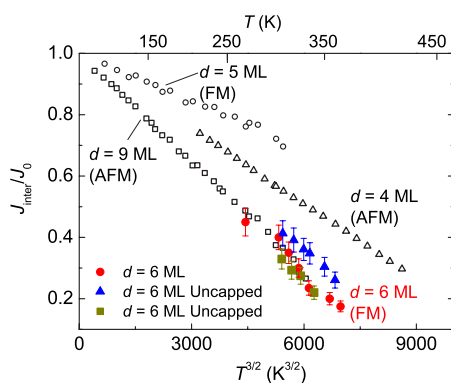
FIG. 9. (Color online) Normalized J_{inter} vs $T^{1.5}$ for different spacer thickness. The data points for the thicknesses of 4, 5, and 9 ML were taken from Schwieger *et al.* (Ref. [12]), and were obtained from the extrapolation of the shift between the H_{res} of Co and the optical mode.

FIG. 10. (a) Fit parameter A vs spacer thickness. (b) J_0 vs spacer thickness. The dashed curves are mere guides to the eye.

FM coupled layers is stronger than that for the AFM coupled layers. Moreover, as expected, there is a stronger decrease with $T^{3/2}$ for larger spacer thicknesses.

Figure 10 shows the connection between the scaling parameter A and the J_0 with relation to the spacer thickness. Figure 10(a) shows the values of A from Eq. (1) vs spacer thickness. Figure 10(b) shows J_0 vs spacer thickness. The data for the 4, 5, and 9 ML have been obtained from an analysis of the data given in Refs. [12] and [16]. The dashed lines are guides to the eye meant to show the trend in the data. Several points can be noted from this figure. Large values of A imply severe suppression of coupling due to temperature. The trends in Fig. 10 are an experimental evidence of the trends predicted by Schwieger and Nolting[14] reproduced in Fig. 2(b). The larger the J_0 value, the weaker is the temperature dependence. A qualitative interpretation of the theoretical prediction can be easily given. The IEC strength between the two ferromagnetic layers is in competition with the thermal energy kT. For strong coupling between FM1 and FM2, the thermal energy can be neglected and elevated temperatures would have little effect on J_{inter}. On the other hand, for vanishing IEC between the two ferromagnetic films, the thermal energy and resulting spin-wave excitations become very important. Hence, it is straightforward that the parameter A in Eq. (1) increases for small IEC and decreases for stronger IEC. The data shown in Fig. 10 confirms this theoretical prediction where the trend shown by the fit parameter A is opposite to that shown by J_0. Another feature is that there is a definite oscillation in A, which indicates that there is a larger role of the spin-wave excitation than of the spacer in the temperature dependence.[14] A linear
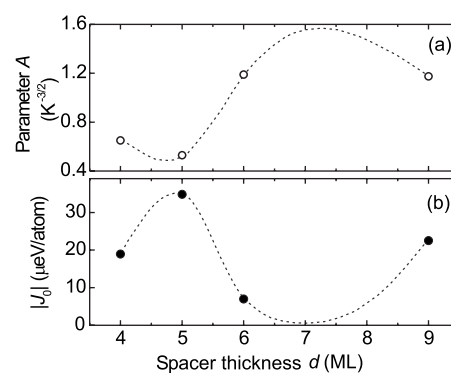
dependence would, on the other hand, have been a signature of the spacer effects.

V. CONCLUSIONS

An investigation into the temperature dependence of J_{inter} was undertaken through the study of ferromagnetic resonance positions in Ni/Cu/Co trilayer systems. The spacer thickness was chosen so that it was in the ultrathin limit and also gave a weak exchange coupling between the two films, a regime important for the fundamental understanding of $J_{inter}(T)$. The interlayer exchange parameter J_{inter} was evaluated entirely from the angular dependence of the FMR positions of the optical and acoustic modes. The fit parameters for the temperature dependence were compared with the extrapolated J_0 values and spacer thicknesses. The scaling parameter A was found to be neither independent nor a linear function of d, as would have been expected from a dominant interface effect or spacer electronic band structure contribution. Instead, the oscillations in A give an experimental verification of the theory forwarded by Schwieger and Nolting.[14] It is a clear conclusion that the excitation of spin waves or in other words, the creation of thermal magnons is the dominant cause of the temperature dependence of J_{inter} in FM and AFM coupled trilayers.

*Current address: Magnetics and Magnetic Materials Laboratory, Colorado State University, Fort Collins, Colorado 80523.

†Permanent address: Surface Physics Laboratory, Fudan University, Shanghai 200433, People's Republic of China.

‡Corresponding author. FAX: +49 30 838-55048; bab@physik.fu-berlin.de; URL: http://www.physik.fu-berlin.de/~bab/

[1] M. D. Stiles, in *Ultrathin Magnetic Structures III*, edited by B. Heinrich and J. A. C. Bland (Springer-Verlag, Heidelberg,

2005), p. 99.

[2] K. B. Hathaway, in *Ultrathin Magnetic Structures II*, edited by B. Heinrich and J. A. C. Bland (Springer-Verlag, Heidelberg, 1994).

[3] J. Lindner, C. Rüdt, E. Kosubek, P. Poulopoulos, K. Baberschke, P. Blomquist, R. Wäppling, and D. L. Mills, Phys. Rev. Lett. **88**, 167206 (2002).

[4] Z. Celinski, B. Heinrich, J. F. Cochran, W. B. Muir, A. S. Arrott, and J. Kirschner, Phys. Rev. Lett. **65**, 1156 (1990).

[5] D. M. Edwards, J. Mathon, R. B. Muniz, and M. S. Phan, Phys. Rev. Lett. **67**, 493 (1991).

[6] Z. Zhang, L. Zhou, P. E. Wigen, and K. Ounadjela, Phys. Rev. Lett. **73**, 336 (1994).

[7] N. S. Almeida, D. L. Mills, and M. Teitelman, Phys. Rev. Lett. **75**, 733 (1995).

[8] J. Lindner, E. Kosubek, P. Poulopoulos, K. Baberschke, and B. Heinrich, J. Magn. Magn. Mater. **240**, 220 (2002).

[9] B. Heinrich, Z. Celinski, L. X. Liao, M. From, and J. F. Cochran, J. Appl. Phys. **75**, 6187 (1994).

[10] A. Layadi and J. O. Artman, J. Magn. Magn. Mater. **92**, 143 (1990).

[11] S. Schwieger, J. Kienert, K. Lenz, J. Lindner, K. Baberschke, and W. Nolting, J. Magn. Magn. Mater. **310**, 2301 (2007).

[12] S. Schwieger, J. Kienert, K. Lenz, J. Lindner, K. Baberschke, and W. Nolting, Phys. Rev. Lett. **98**, 057205 (2007).

[13] P. Bruno, Phys. Rev. B **52**, 411 (1995).

[14] S. Schwieger and W. Nolting, Phys. Rev. B **69**, 224413 (2004).

[15] B. Heinrich, in *Ultrathin Magnetic Structures II*, edited by B. Heinrich and J. A. C. Bland (Springer-Verlag, Heidelberg, 1994).

[16] J. Lindner and K. Baberschke, J. Phys.: Condens. Matter **15**, R193 (2003).

[17] P. Gambardella, S. Rusponi, M. Veronese, S. S. Dhesi, C. Grazioli, A. Dallmeyer, I. Cabria, R. Zeller, P. H. Dederichs, K. Kern *et al.*, Science **300**, 1130 (2003).

[18] K. Baberschke, Appl. Phys. A: Mater. Sci. Process. **62**, 417 (1996).

[19] K. Lenz, E. Kosubek, T. Tolinski, J. Lindner, and K. Baberschke, J. Phys.: Condens. Matter **15**, 7175 (2003).

[20] P. Srivastava, F. Wilhelm, A. Ney, M. Farle, H. Wende, N. Haack, G. Ceballos, and K. Baberschke, Phys. Rev. B **58**, 5701 (1998).

[21] E. Holmström *et al.*, Phys. Rev. Lett. **97**, 266106 (2006).

[22] B. Heinrich, in *Ultrathin Magnetic Structures III*, edited by B. Heinrich and J. A. C. Bland (Springer-Verlag, Heidelberg, 2003).

[23] Y. Li and K. Baberschke, Phys. Rev. Lett. **68**, 1208 (1992).

[24] J. Smit and H. G. Beljers, Philips Res. Rep. **10**, 113 (1955).

[25] M. Tischer, O. Hjortstam, D. Arvanitis, J. Hunter-Dunn, F. May, K. Baberschke, J. Trygg, J. M. Wills, B. Johansson, and O. Eriksson, Phys. Rev. Lett. **75**, 1602 (1995).

[26] R. Hammerling, J. Zabloudil, P. Weinberger, J. Lindner, E. Kosubek, R. Nünthel, and K. Baberschke, Phys. Rev. B **68**, 092406 (2003).